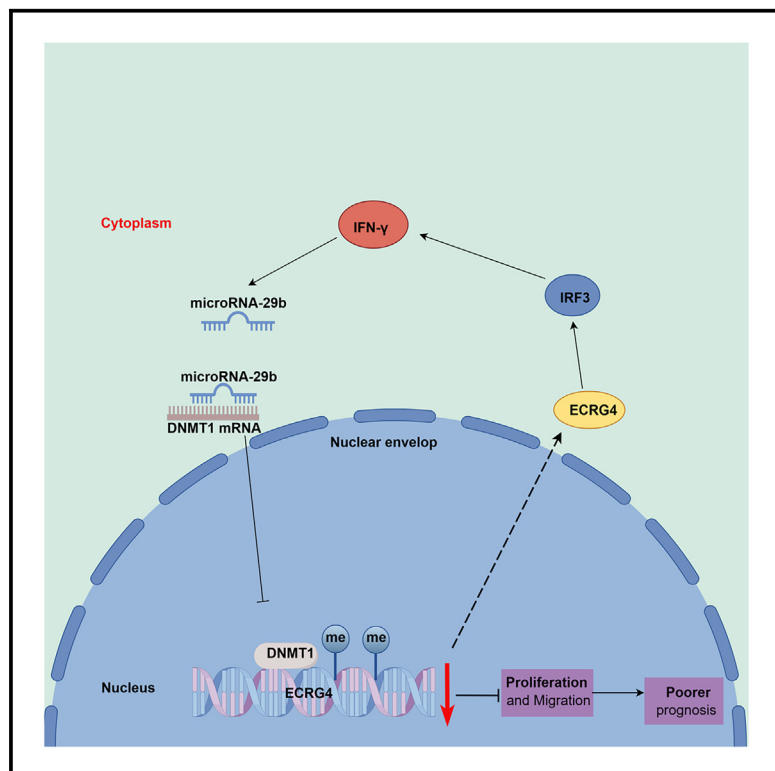# Downregulation of ECRG4 by DNMT1 promotes EC growth via IRF3/IFN-γ/miR-29b/DNMT1/ECRG4 positive feedback loop

Graphical abstract

Authors

Ke Yang, Shuaining Chai, Helong Song, Sinan Cao, Fangmiao Gao, Chenxuan Zhou, Linwei Li

Correspondence

lilinweillw@126.com

In brief

Molecular mechanism of gene regulation; Epigenetics; Cancer

Highlights

- ECRG4 promoter is highly methylated and downregulated in esophageal carcinoma

- DNMT1 mediated the epigenetic downregulation of ECRG4

- Downregulation of ECRG4 promotes esophageal carcinoma growth

iScience

Article

Downregulation of ECRG4 by DNMT1 promotes EC growth via IRF3/IFN-γ/miR-29b/ DNMT1/ECRG4 positive feedback loop

Ke Yang,[1] Shuaining Chai,[2] Helong Song,[2] Sinan Cao,[2] Fangmiao Gao,[1] Chenxuan Zhou,[1] and Linwei Li[1,2,3,*]

[1]Department of Oncology, Zhengzhou University People's Hospital, Henan Provincial People's Hospital, Zhengzhou, 450003 Henan, China
[2]Department of Oncology, Henan University People's Hospital, Henan Provincial People's Hospital, Zhengzhou, 450003 Henan, China
[3]Lead contact
*Correspondence: lilinweillw@126.com
https://doi.org/10.1016/j.isci.2024.111614

SUMMARY

Esophageal carcinoma (EC) is one of the most common malignant tumors in the world. ECRG4 has been recently discovered to be downregulated in EC. However, the mechanism leading to reduced expression of ECRG4 in esophageal cancer remains obscure. Here, we found that ECRG4 expression was significantly downregulated in EC tissues and cell lines. ECRG4 overexpression led to a significant decrease in proliferation *in vitro* and *in vivo*. Mechanistically, ECRG4 can activate IRF3/IFN-γ pathway. IFN-γ can promote the expression of miR-29b. MiR-29b reduces the expression of DNMT1. DNMT1 may affect the expression of ECRG4 by affecting the methylation of ECRG4 promoter. These results reveal ECRG4/IRF3/IFN-γ/miR-29b/DNMT1 positive feedback loop in esophageal carcinoma cells, which may become a potential therapeutic target for esophageal carcinoma.

INTRODUCTION

Esophageal carcinoma (EC) is one of the most common malignant tumors in the world. According to Global Cancer Statistics, in 2020, the incidence rate of EC was about 3.1%, ranking seventh in all kinds of carcinoma; the mortality rate of carcinoma was about 5.5%, ranking sixth in all kinds of carcinoma.[1] EC has two histological types, esophageal squamous carcinoma and esophageal adenocarcinoma. Esophageal adenocarcinoma accounted for 10% of EC, mainly in the western countries. Esophageal squamous cell carcinoma accounts for about 90% of esophageal cancers each year. The high-incidence regions include Eastern to Central Asia.[2,3] China is a particularly high-risk area where EC cases account for more than half of the world.[4] Therefore, an understanding of the molecular mechanisms underlying esophageal cancer progression could provide new therapeutic targets for the development of EC.

Esophageal cancer-related gene 4 (ECRG4) was originally cloned and identified from normal human esophageal epithelium in 1998.[5] ECRG4 often acts as a tumor suppressor gene and is frequently hypermethylated at the promoter region.[6] Meanwhile, restoring ECRG4 expression represses cell proliferation and invasiveness.[7] ECRG4 also can act as an indicator for predicting cancer patient prognosis and a determinant of chemotherapy resistance.[8,9] In EC, ECRG4 is a novel candidate tumor suppressor gene.[10] ECRG4 can inhibit cell growth in EC.[11]

Epigenetics is defined as changes in gene expression or cell phenotype that can be inherited by some mechanism without altering the DNA sequence. DNA methylation, histone structure change and microRNA regulation of genes are important carriers of epigenetic information.[12] DNA methylation is one of the important epigenetic modification. Transcriptional silencing by CpG island methylation is a prevalent mechanism of gene suppression in cancers, and DNA methyltransferase 1 (DNMT1) is required to maintain CpG methylation and aberrant gene silencing in human cancer cells.[13] Silencing DNMT1 restores tumor suppressor gene expression through the reversal of DNA hypermethylation.[14] Treatment breast cancer with DNMT1 inhibitor 5-Azacytidine (5-aza-dC) suppresses tumorigenesis and tumor growth along with increased expression of FOXO3a.[15] In esophageal squamous cell carcinoma, silencing DNMT1 inhibits proliferation, metastasis and invasion.[16]

In our present study, we validated the downregulatory expression of ECRG4 in EC tissues and cells. Furthermore, ECRG4 inhibited the EC cell growth *in vitro* and *in vivo*. Mechanistically, proteomics results show that ECRG4 can activate IRF3/IFN-γ pathway. IFN-γ can promote the expression of miR-29b. MiR-29b reduces the expression of DNMT1. DNMT1 can affect the expression of ECRG4 by affecting the methylation of ECRG4 promoter. Therefore, ECRG4/IRF3/IFN-γ/miR-29b/DNMT1 positive feedback axis might provide potential targets for EC.

RESULTS

ECRG4 activates the IRF3/IFN-γ pathway

To further investigate the role of ECRG4 in EC, we examined the expression of ECRG4 in normal esophageal squamous epithelial cells (HEEC) and EC cell lines, including EC9706 and EC-18 by
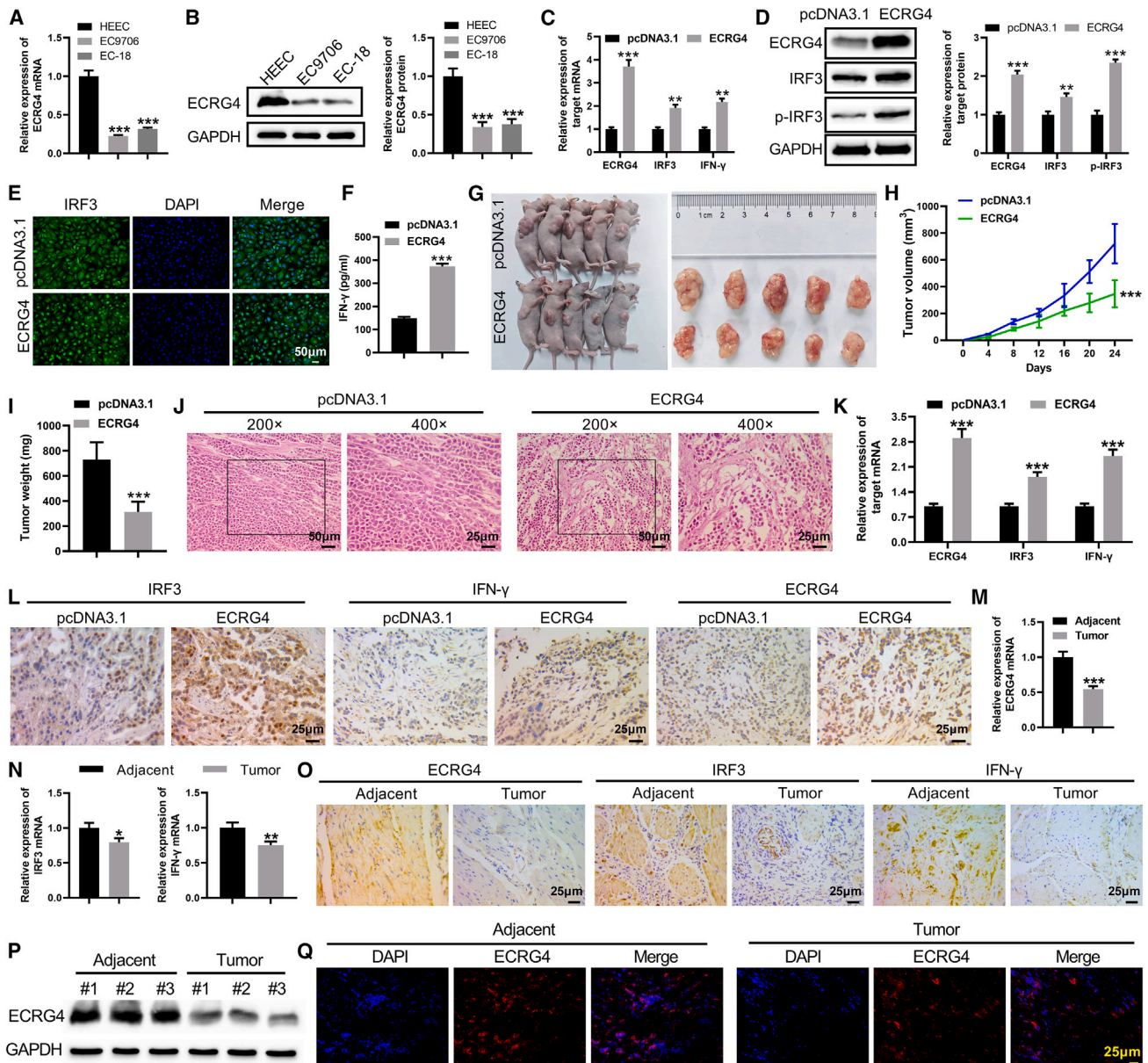
Figure 1. ECRG4 activates the IRF3/IFN-γ pathway

(A) qRT-PCR was used to measure ECRG4 mRNA expression in different cell lines.

(B) The protein levels of ECRG4 were detected in different cell lines by Western blot.

(C) qRT-PCR was used to measure IRF3 and IFN-γ mRNA expression in different cell lines.

(D) Western blot was used to measure *p*-IRF3 and IRF3 expression in EC9706 cells transfected with ECRG4 plasmid.

(E) Immunofluorescence was used to analyze localization of IRF3.

(F) Elisa assay was used to measure IFN-γ protein expression in supernatant.

(G–I) EC9706 cells with stable expression of an ECRG plasmid or Vector were subcutaneously injected into nude mice. The mice were randomly divided into two groups: Vector group and ECRG plasmid group. Tumor volumes were measured on the days as indicated. After 24 days, the mice were sacrificed and tumor weights were examined.

(J) H&E staining showed that morphology changes in EC9706 cells.

(K) qRT-PCR was used to measure IFR3 and IFN-γ mRNA in the tumor specimens from the mice.

(L) Immunohistochemistry for IFR3 and IFN-γ in the tumor specimens from the mice.

(M) ECRG4 mRNA expression in 10 pairs of esophageal cancer tissues and adjacent non-tumor tissues, was determined by qRT-PCR.

(N) IFR3 and IFN-γ mRNA expression in 10 pairs of esophageal cancer tissues and adjacent non-tumor tissues was determined by qRT-PCR.

qRT-PCR and Western blot analysis. We found that the expression of ECRG4 was higher in HEEC cells than that in EC9706 and EC-18 cells (Figures 1A and 1B). To get the potential pathway regulated by ECRG4, we overexpressed ECRG4 in EC cell line EC9706 cells and carried out the proteomics analysis. Proteomic analysis results showed that the IRF3 was upregulated and interferon pathway was activated in the ECRG4 overexpressed EC9706 cells (Figure S1). To confirm this result, we further analyzed whether ECRG4 affects IRF3 and IFN-γ expression in EC cells. As shown in Figure 1C, ECRG4 overexpression increased expression of IRF3 and IFN-γ. Western blot also showed the expression of p-IRF3 was increased when transfected with ECRG4 plasmid in EC9706 cells (Figure 1D). In addition, IF exhibited ECRG4 overexpression can promote the nuclear translocation of IRF3 (Figure 1E). As a secreted protein, IFN-γ was also measured by Elisa assay. The level of IFN-γ protein was higher in ECRG4 overexpression group than that in the control group (Figure 1F). To explore the role of ECRG4 in the tumorigenesis of EC in vivo, we implanted equal numbers of negative control and ECRG4 overexpressing EC9706 and EC18 cells into nude mice and monitored tumor growth for 24 days (Figure S2A) (Figure 1G). Tumor growth curve analysis suggested that ECRG4 overexpression delayed EC9706 cell and EC18 associated tumor progression (Figure S2B) (Figure 1H). The tumor weight was also lighter in the ECRG4 overexpression group than in the control group (Figure S2C) (Figure 1I). H&E staining showed ECRG4 overexpression xenografts exhibited morphologic characteristics of well differentiated carcinoma and decreased cell mitosis (Figure S2D) (Figure 1J). qRT-PCR and IHC results showed that IRF3 and IFN-γ were upregulated in the ECRG4 overexpression tumor specimens from the mice (Figure S2E) (Figures 1K and 1L). To explore the clinical relevance of ECRG4 in EC, we also evaluated the expression of ECRG4, IRF3 and IFN-γ in human EC and normal tissues by qRT-PCR and immunohistochemical staining. The results showed that the expression of ECRG4, IRF3, and IFN-γ was reduced in EC tissues compared with that in normal tissues (Figures 1M–1O). The Western blot and IF results also showed that the expression of ECRG4 was reduced in EC tissues compared with that in normal tissues (Figures 1P and 1Q).

ECRG4 inhibits tumor cell proliferation and tumor growth through IRF3/IFN-γ pathway

IFN-γ can increase the expression of miR-29b in CD4^{+} T cells.[17] First, we analyzed the miR-29b expression in human EC and normal tissues by qRT-PCR. The miR-29b expression was decreased in human EC than in normal tissues (Figure 2A). qRT-PCR results show the expression of miR-29b was increased when transfected with ECRG4 plasmid in EC9706 cells (Figure 2B). We synthesized three sequences of IRF3 siRNA and chose the one that has the best knockdown efficiency sequence for further study (Figure S3A). Because ECRG4 regulates both IRF3 and IFN-γ in EC cells, we explored whether the regulation

of IFN-γ by ECRG4 involves IRF3. Figures 2C–2F shows ECRG4 can increase the expression of IFN-γ at the mRNA and protein level, while the transfection of IRF3 siRNA can reverse this effect. This result shows that ECRG4 may regulate the IFN-γ expression through IRF3. As a transcription factor, IRF3 can be translocated to the nucleus by ECRG4 overexpression (Figure 2G). The above results show that ECRG4 may upregulate IFN-γ by the nucleus translocation of IRF3. Next, we tested the proliferation capacity and apoptosis rate of the cells transfected ECRG4 plasmid or cotransfected ECRG4 plasmid and IRF3 siRNA. The CCK-8 assay showed that the cell proliferation rate was significantly reduced in EC9706 cells with overexpression of ECRG4, but was rescued by IRF3 knockdown (Figure 2H). Colony formation assays also showed that the colony-forming ability was significantly reduced in ECRG4 overexpression cells compared with counterpart cells, but was rescued by IRF3 knockdown (Figures 2I and 2J). Flow cytometry analysis shows ECRG4 plasmid can increase the apoptosis of EC9706, while IRF3 siRNA can reverse this effect (Figure 2K). qRT-PCR also shows ECRG4 plasmid can increase the miR-29b expression level, while IRF3 siRNA can reverse this effect (Figure 2L).

IFN-γ promotes the expression of miR-29b and inhibits tumor growth

IFN-γ induces mitochondria-mediated apoptosis and acts as a tumor suppressor.[18] IFN-γ also increased the expression of miR-29b in CD4^{+} T cells.[17] As shown in Figure 3A, IFN-γ decreased EC9706 cell viability as evidenced by CCK-8 assays. IFN-γ dramatically decreased the clone number of EC9706 cells (Figure 3B). IFN-γ also increased the mRNA and protein of ECRG4 and miR-29b mRNA expression in EC9706 cells, indicating there might be a positive feedback loop between IFN-γ and ECRG4(Figures 3C and 3D). To further determine the antitumor effects of IFN-γ, an ECRG4 xenograft model was established. IFN-γ significantly inhibited tumor growth, as demonstrated by the significantly reduced tumor volumes and weights compared to the control group (Figures 3E–3G). H&E staining showed that the histopathology of tumors formed in the IFN-γ xenografts exhibited morphologic characteristics of well differentiated carcinoma and decreased cell mitosis (Figure 3H). QRT-PCR shows miR-29b was upregulated in the IFN-γ treatment tumor specimens from the mice (Figure 3I).

DNMT1 can affect the expression of ECRG4 by affecting the methylation of ECRG4 promoter

The low expression of ECRG4 is associated with hypermethylation in the promoter region and plays an important role in the malignancy of cancer.[19,20] We first analyzed the methylation level in human EC and normal tissues. 5mC level in human EC was higher than that in the normal tissue (Figure 4A). Further, methylation of ECRG4 was higher in human EC tumors compared with their corresponding controls (Figure 4B). DNA methyltransferase mediated epigenetic silencing of tumor suppressor genes.

(O) ECRG4, IRF3and IFN-γ protein expression in 10 pairs of esophageal cancer tissues and adjacent non-tumor tissues, detected by immunocytochemistry.
(P) The protein levels of ECRG4 were detected in 3 pairs of esophageal cancer tissues and adjacent non-tumor tissues by Western blot.
(Q) Immunofluorescence was used to analyze the ECRG4 protein in esophageal cancer tissues and adjacent non-tumor tissues. The values are presented as mean ± s.d. p values are calculated by a two-tailed Student's t test or one-way ANOVA with Tukey's post hoc analysis. *p < 0.05, **p < 0.01, ***p < 0.001.
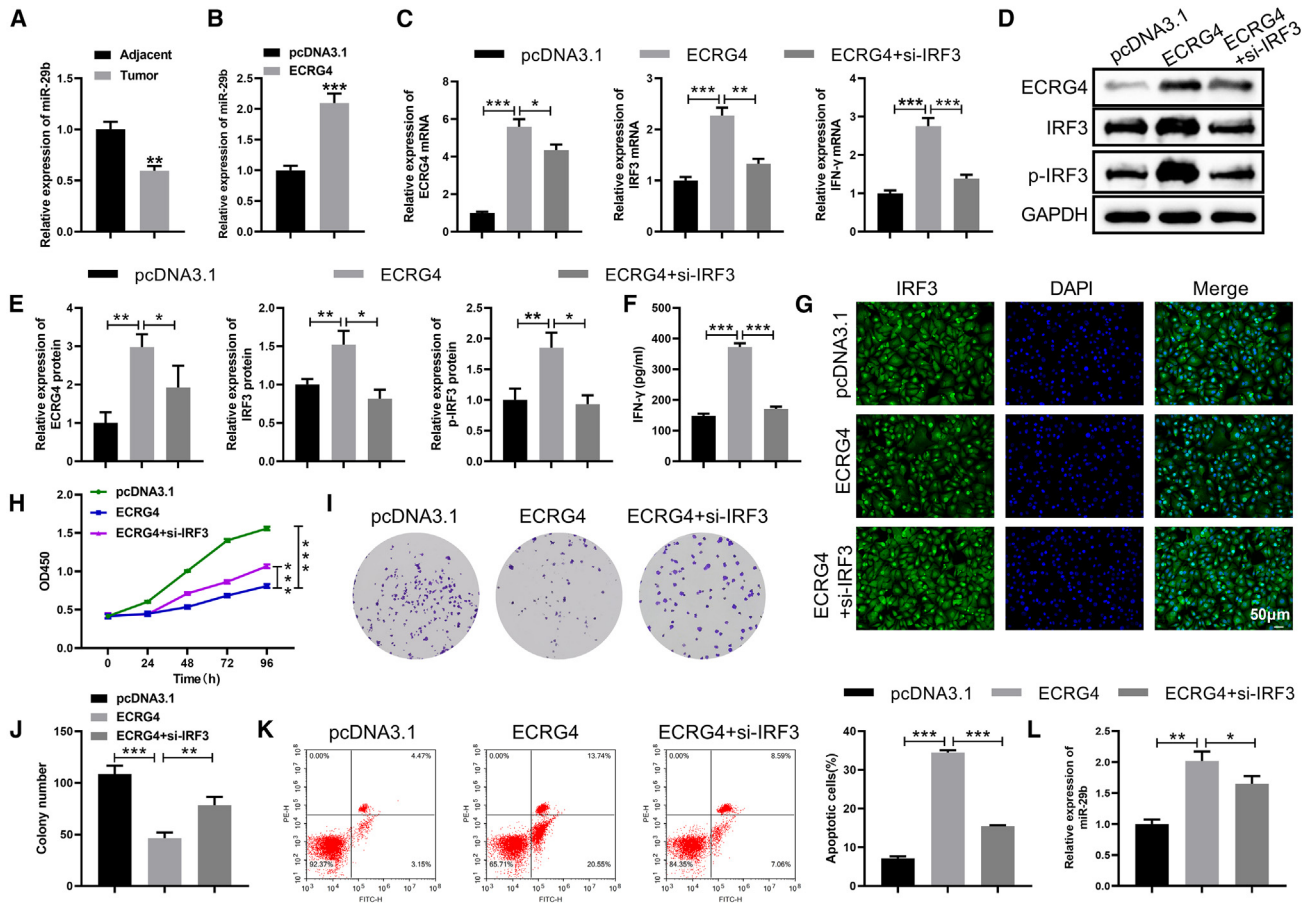
Figure 2. ECRG4 inhibited tumor cell proliferation and tumor growth through IRF3/IFN-γ pathway

(A) MiR-29b mRNA expression in 10 pairs of esophageal cancer tissues and adjacent non-tumor tissues, determined by qRT-PCR.

(B) qRT-PCR was used to measure miR-29b mRNA expression in EC9706 cells transfected with ECRG4 plasmid.

(C) qRT-PCR was used to measure IFN-γ mRNA expression in EC9706 cells transfected with ECRG4 plasmid or cotransfected with ECRG4 plasmid and IRF3 siRNA.

(D and E) Western blot was used to measure IRF3 and p-IRF3 protein expression in EC9706 cells transfected with ECRG4 plasmid or cotransfected with ECRG4 plasmid and IRF3 siRNA.

(F) Elisa was used to measure IFN-γ protein in EC9706 cells transfected with ECRG4 plasmid or cotransfected with ECRG4 plasmid and IRF3 siRNA.

(G) Immunofluorescence was used to analyze localization of IRF3.

(H) CCK 8 assay was used to detect cell proliferation of in EC9706 cells transfected with ECRG4 plasmid or cotransfected with ECRG4 plasmid and IRF3siRNA.

(I and J) Plate cloning assay was used to detect cell proliferation of EC9706 cells transfected with ECRG4 plasmid or cotransfected with ECRG4 plasmid and IRF3 siRNA.

(K) Flow cytometry was used to detect cell apoptosis of EC9706 cells transfected with ECRG4 plasmid or cotransfected with ECRG4 plasmid and IRF3 siRNA.

(L) qRT-PCR was used to detect miR-29b mRNA expression in EC9706 cells transfected with ECRG4 plasmid or cotransfected with ECRG4 plasmid and IRF3 siRNA. p values are calculated by a two-tailed Student's t test or two-way ANOVA with Tukey's post hoc analysis. The values are presented as mean ± s.d. $^{*}p < 0.05$, $^{**}p < 0.01$, $^{***}p < 0.001$.

DNMT1 was the highest in human EC among three DNMT enzymes than that in the normal tissue (Figures 4C and 4D). Figure 4E shows that DNMT can affect the expression of ECRG4 through DNMT activity. To prove whether DNMT1-mediated hypermethylation of ECRG4 was responsible for downregulating ECRG4, we carried out ChIP analysis. We found that the ECRG4 mRNA immunoprecipitated by DNMT1 antibody was significantly increased after transfection of ECRG4 and DNMT1 plasmid compared with ECRG4 overexpression group (Figure 4F). Further, methylation of ECRG4 was higher after transfection of ECRG4 and DNMT1 plasmid compared with ECRG4 over-

expression group (Figure 4G). qRT-PCR and western blot showed that mRNA and protein of ECRG4 were lower after transfection of ECRG4 and DNMT1 plasmid compared with ECRG4 overexpression group (Figures 4H and 4I). These results showed that DNMT1 can affect the expression of ECRG4 by affecting the methylation of ECRG4 promoter. Because DNMT1-mediated methylation downregulated ECRG4 expression, we next tested whether pharmacological inhibition of DNMTs could suppress tumorigenesis and tumor growth by regulating ECRG4. We found that treatment with DNMT inhibitor 5-aza-dC or ECRG4 plasmid significantly inhibited the proliferation of EC9706 cells,
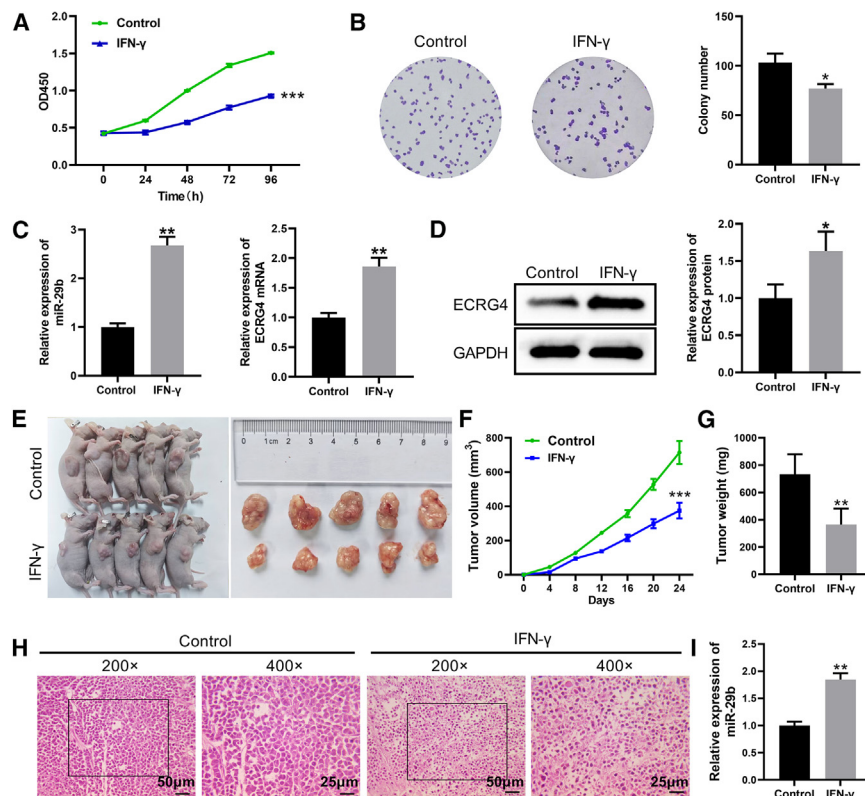
Figure 3. IFN-γ promoted the expression of miR-29b and inhibited tumor growth

(A) The cell viability of EC9706 cells treated with IFN-γ was assessed by CCK-8 assay.

(B) The cell viability of EC9706 cells treated with IFN-γ was assessed by plate cloning assay.

(C) qRT-PCR was used to measure miR-29b mRNA expression in EC9706 cells treated with IFN-γ.

(D) Western blot was used to measure ECRG4 protein expression in EC9706 cells treated with IFN-γ.

(E) EC9706 were subcutaneously injected into female nude mice. The mice were randomly divided into two groups.

(F) Tumor volumes were measured on the days as indicated.

(G) After 24 days, the mice were sacrificed and tumor weights were examined.

(H) H&E staining showed that morphology changes in EC9706 cells.

(I) MiR-29b mRNA expression in IFN-γ treated tumor specimens determined by qRT- PCR. The values are presented as mean ± s.d. p values are calculated by a two-tailed Student's t test. $*p < 0.05$, $**p < 0.01$, $***p < 0.001$.

while cotransfection of ECRG4 and DNMT1 plasmid can reverse this effect (Figures 4J and 4K). The pro-apoptosis effect of DNMT inhibitor 5-aza-dC or ECRG4 plasmid overexpression was reversed by the cotransfection of ECRG4 and DNMT1 plasmid (Figure 4L).

MiR-29b downregulates DNMT1 expression, thereby inhibiting tumor cell proliferation

Research shows that miR-29b downregulates DNMT1expression in acute myeloid leukemia.[18] First, we found that miR-29b may affect the expression of ECRG4 by affecting the methylation of ECRG4 promoter. This process may be mediated by the enzyme DNMT1 (Figures S3B and 5A–5C). We overexpressed miR-29b mimics in EC9706 cells and found that EC9706 cells transfected with miR-29b mimics showed a significant reduction in OD values and colony formation (Figures 5D and 5E). Flow cytometry analysis was utilized to evaluate the induction of apoptosis in cells with the expression of miR-29b. Flow cytometry showed that miR-29b mimics induce apoptosis in EC9706 cells (Figure 5F). MiR-29b also increased the mRNA and protein of IFN-γ in EC9706 cells, indicating there might be a positive feedback loop between miR-29b and IFN-γ (Figures 5G and 5H).

MiR-29b upregulates ECRG4 expression, thereby inhibiting tumor cell proliferation

MiR-29b inhibitor can decrease the ECRG4 mRNA and protein level, possibly due to the increased methylation of the ECRG4 promoter (Figures 6A–6C). Next, we investigated the role of

miR-29b and ECRG4 on the proliferation of EC9706 cells. MiR-29b inhibitor can increase the OD values and colony formation of EC9706, while ECRG4 overexpression can reverse this effect (Figures 6D and 6E). Flow cytometry analysis shows ECRG4 overexpression can increase the apoptosis of EC9706, while miR-29b inhibitor can reverse this effect (Figure 6F). ECRG4 overexpression can increase the IFN-γ mRNA and protein level, while transfection of miR-29b inhibitor can reverse this effect (Figures 6G and 6H). All these results show that miR-29b upregulates ECRG4 expression, thereby inhibiting tumor cell proliferation.

MiR-29b downregulates DNMT1 expression, thereby inhibiting tumor cell proliferation *in vivo*

We also evaluated the effects of miR-29b on the growth of EC9706 cell xenografts in mice. EC9706 cells were transfected with control lentivirus, or miR-29b lentivirus. Cells were implanted subcutaneously into the mouse flanks. Finally, the tumor volume and tumor weight were used to evaluate the effect of ECRG4 (Figure 7A). We observed a significant decrease in the size and weight of the tumors in the miR-29b mimic xenografts (Figures 7B and 7C). H&E staining showed that the histopathology of tumors formed in the miR-29b xenografts exhibited morphologic characteristics of well differentiated carcinoma and decreased cell mitosis (Figure 7D). Further, miR-29b can decrease the methylation level of ECRG4 (Figure 7E). qRT-PCR and IHC results further verify the results that miR-29b downregulates DNMT1 expression and upregulates ECRG4 expression. (Figures 7F and 7G). All these results show that miR-29b downregulates DNMT1 expression, thereby inhibiting tumor cell proliferation.
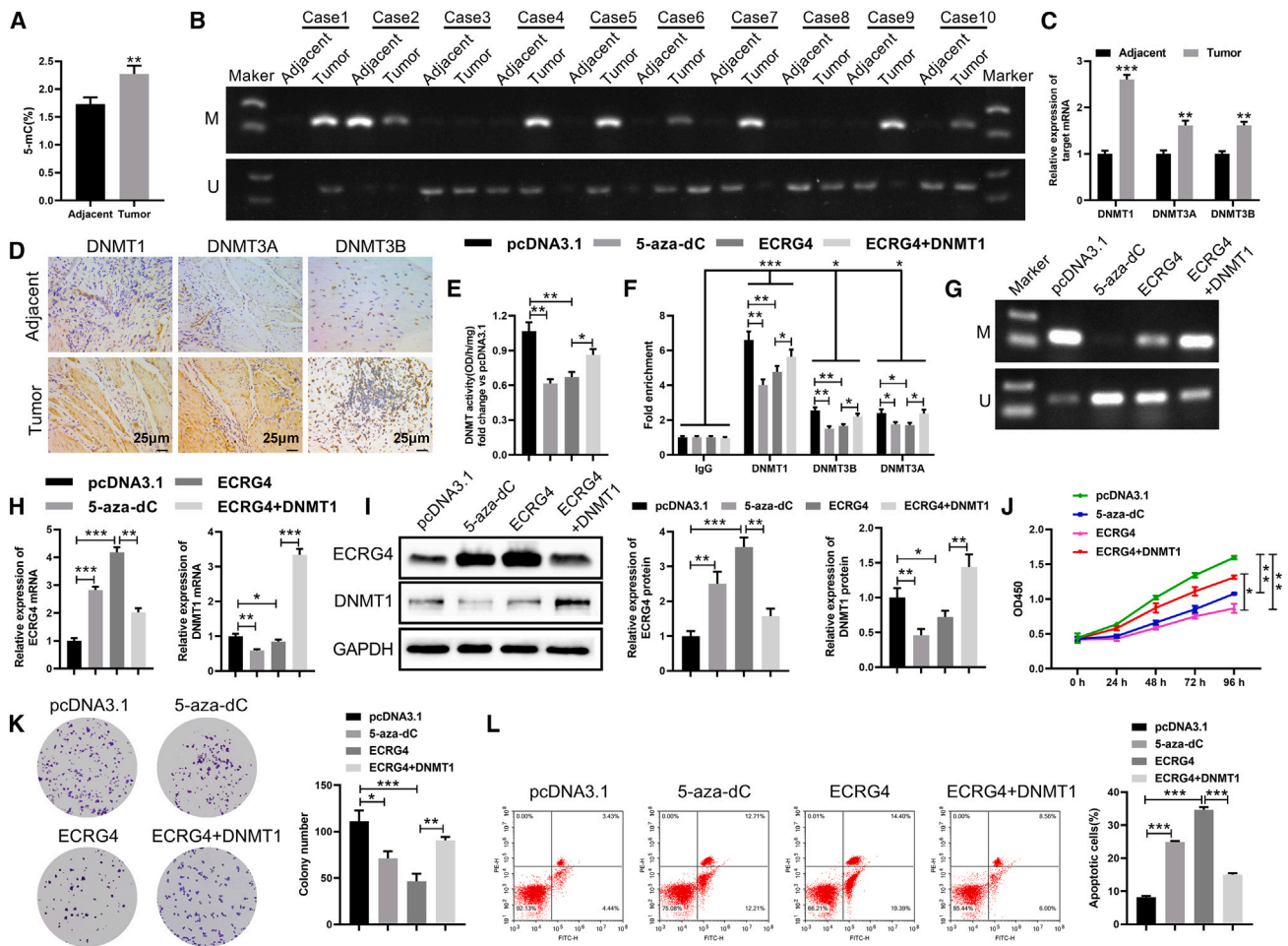
Figure 4. DNMT1 affects the expression of ECRG4 by affecting the Methylation of ECRG4 promoter

(A) Elisa assay to test the global DNA methylation using 100 ng of genomic DNA isolated from 10 pairs of esophageal cancer tissues and adjacent non-tumor tissues.

(B) Methylation-specific PCR was performed to evaluate the ECRG4 DNA methylation status from 10 pairs of esophageal cancer tissues and adjacent non-tumor tissues.

(C) DNMT mRNA expression in 10 pairs of esophageal cancer tissues and adjacent nontumor tissues, was determined by qRT-PCR.

(D) DNMT protein expression in 10 pairs of esophageal cancer tissues and adjacent non-tumor tissues was detected by immunocytochemistry.

(E) Colorimetric DNMT activity assay was performed using nuclear extracts from EC9706 cells treated with the indicated agents. DNMT activity (OD/h/mg) is expressed as fold change vs. control.

(F) ChIP-qPCR analysis of ECRG4 promoter.

(G) Methylation specific PCR was performed to evaluate the ECRG4 DNA methylation changes under different treatments in EC9706 cells.

(H) qRT-PCR was used to measure ECRG4 mRNA expression in EC9706 cells with different treatments.

(I) Western blot was used to measure ECRG4 expression in EC9706 cells under different treatments.

(J and K) CCK-8 and plate cloning assay were used to detect cell proliferation ability.

(L) Flow cytometry was used to detect apoptosis. The values are presented as mean ± s.d. p values are calculated by two-tailed Student's t test or two-way ANOVA with Tukey's post hoc analysis. $*p < 0.05$, $**p < 0.01$, $***p < 0.001$.

DISCUSSION

EC is one of the most common malignant tumors in the world. In this study, we found that the expression of ECRG4 was remarkably downregulated in EC tissues and cells. ECRG4 inhibited EC cell proliferation *in vitro* and *in vivo*. Mechanistically, we found that ECRG4 can activate IRF3/IFN-γ pathway. IFN-γ can promote the expression of miR-29b. miR-29b reduces the expression of DNMT1. DNMT1 can affect the

expression of ECRG4 by affecting the methylation of ECRG4 promoter.

There are some reports explaining the potential pathway related to ECRG4 in certain cancers. For example, ECRG4 suppresses breast cancer cell via regulating mitosis-associated gene expression and M phase progression of cell cycle in breast cancer.[21] ECRG4 inhibits the malignant phenotype of TCA8113 cells most likely through suppression of lncRNA/MMPs signaling pathway in oral squamous cell carcinoma.[22] ECRG4 inhibits
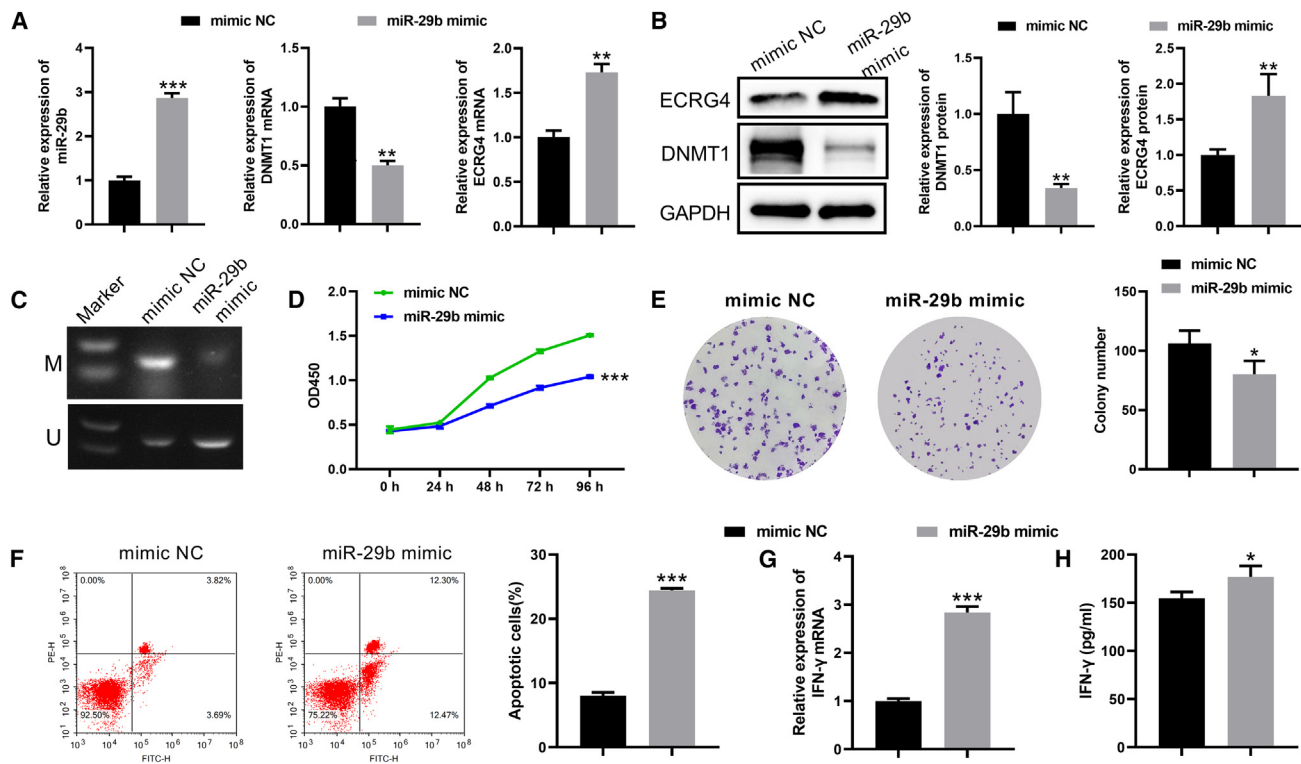
Figure 5. MiR-29b downregulates DNMT1 expression, thereby inhibiting tumor cell proliferation

(A) The EC9706 cells were transfected with miR-29b mimics 50 nM for 4 h, and the DNMT1 and ECRG4 mRNA expression was determined by qRT-PCR.

(B) The EC9706 cells were transfected with miR-29b mimics 50 nM for 4 h, the DNMT1, and ECRG4 protein expression were determined by Western blot.

(C) Methylation-specific PCR was performed to evaluate the ECRG4 DNA methylation changes under different treatment in EC9706 cells.

(D) The EC9706 cells were transfected with miR-29b mimic. Proliferation of EC9706 was measured by CCK8.

(E) The EC9706 cells were transfected with miR-29b mimic. Proliferation of EC9706 was measured by plate cloning assay.

(F) EC9706 cells were stained with annexin V and PI and analyzed by flow cytometry.

(G) EC9706 cells were transfected with miR-29b mimics 50 nM for 4 h, the IFN-γ mRNA expression was determined by qRT-PCR.

(H) The EC9706 cells were transfected with miR-29b mimics 50 nM for 4 h, the IFN-γ protein expression was determined by Elisa. The values are presented as mean ± s.d. p values are calculated by a two-tailed Student's t test. *$p < 0.05$, **$p < 0.01$, ***$p < 0.001$.

metastasis by influencing activating the PI3K/AKT/mTOR signaling pathway in nasopharyngeal carcinoma cells.[23] But the pathway regulated by ECRG4 in EC is still unclear. Further studies show that ECRG4 may be related to the immune response. ECRG4 deficiency impairs neutrophil response to an aseptic injury.[24] ECRG4 directly induces the expression of pro-inflammatory factors, including tumor necrosis factor-α (TNF-α) and type-I interferon (IFN).[25] Yang et al. showed that ECRG4 may act as a tumor suppressor by suppressing the AKT/GSK3β/β-catenin signaling pathway in nasopharyngeal carcinoma.[26] In this text, we find ECRG4 was downregulated in EC tissues. IRF3/IFN-γ pathway was activated by ECRG4 overexpression, implying this pathway may be the downstream of ECRG4.

The cGAS-STING pathway is important for cancer. STING activation triggers multiple signaling cascades leading to activation of IRF3.[27] In unstimulated cells, IRF3 is present in the cytoplasm. STING activation results in the phosphorylation of IRF3, leading to its dimerization and nuclear accumulation.[28] IRF3 in tumor-bearing mice can increase the production of

IFNγ.[29] The function of IFN-γ might have an anti-tumor effect. On one hand, IFN-γ contributes to apoptotic cell death.[30,31] On the other hand, IFN-γ can promote the activation of M1-like macrophages, increase CD4$^+$ T and CD8$^+$ T cells, and inhibit the progression of colon cancer, which may provide insight into immunotherapeutic approaches for colon cancer.[32,33] In this text, IFN-γ shows its anti-tumor effect *in vitro* and *in vivo*.

The function of miRNA-29b in cancer is controversial. On one hand, miR-29b may function as tumor suppressor gene. MiR-29b can inhibit cancer cell growth and invasion, reduce angiogenesis, and induce apoptosis.[34–36] MiR-29b can also reverse oxaliplatin-resistance in colorectal cancer potentiating etoposide toxicity.[37] MiR-29b inhibits resistance to methotrexate in osteosarcoma in HeLa cells.[38] MiR-29b could promote radio sensitivity in radioresistant subpopulations of cervical cancer cells.[39] On the other hand, miR-29b may also function as an oncogene. MiR-29b enhances prostate cancer cell invasion independently of MMP-2 expression.[40] MiR-29b enhances cell migration and invasion in
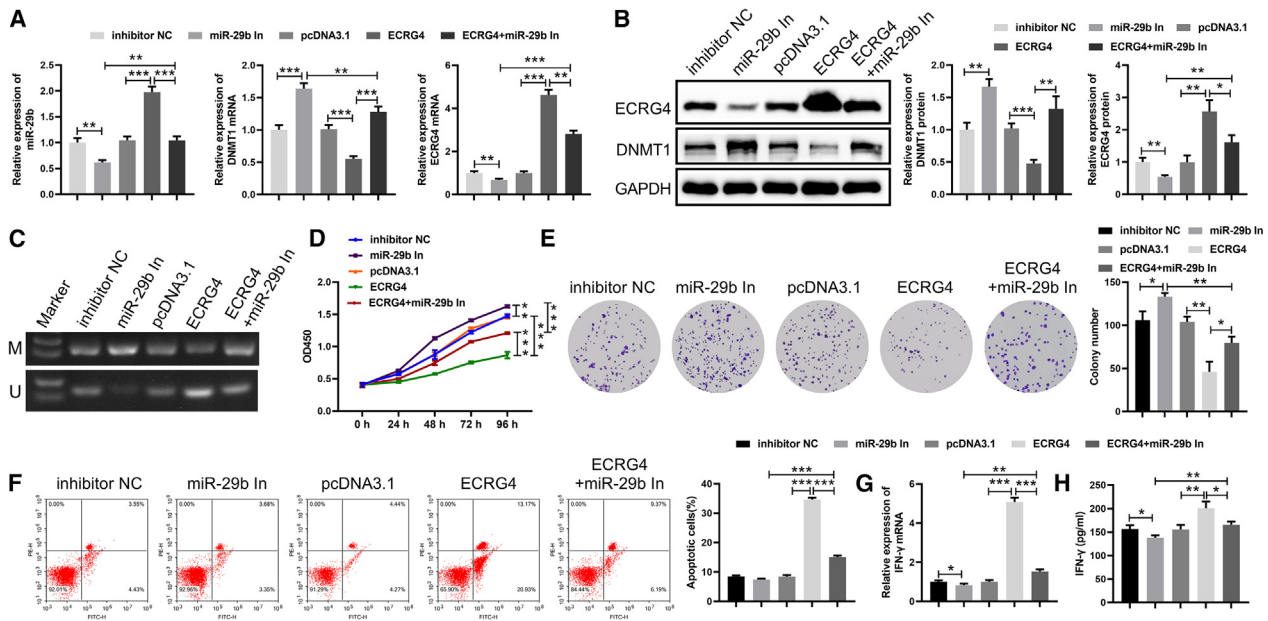
Figure 6. MiR-29b upregulates ECRG4 expression, thereby inhibiting tumor cell proliferation

(A) EC9706 cells were transfected with miR-29b inhibitor or (with) ECRG4 plasmid, the DNMT1and ECRG4 mRNA expression was determined by qRT-PCR.

(B) The EC9706 cells were transfected with miR-29b mimics or (with) ECRG4 plasmid, the DNMT1 and ECRG4 protein expression was determined by Western blot.

(C) Methylation-specific PCR was performed to evaluate the ECRG4 DNA methylation changes under the treatment in EC9706 cells (D) EC9706 cells were transfected with miR-29b inhibitor or (with) ECRG4 plasmid. Proliferation of EC9706 was measured by CCK8.

(E) The EC9706 cells were transfected with miR-29b mimic. The proliferation of EC9706 was measured by plate cloning assay.

(F) The EC9706 cells were stained with annexin V and PI and analyzed by flow cytometry.

(G) The EC9706 cells were transfected with miR-29b inhibitor or (with) ECRG4 plasmid, the IFN-γ mRNA expression was determined by qRT-PCR.

(H) The EC9706 cells were transfected with miR-29b inhibitor or (with) ECRG4 plasmid, the IFN-γ protein expression was determined by Elisa assay. The values are presented as mean ± s.d. p values are calculated by two-way ANOVA with Tukey's post hoc analysis *$p < 0.05$, **$p < 0.01$, ***$p < 0.001$.

nasopharyngeal carcinoma progression by regulating SPARC and COL3A1 gene expression.[41] MiR-29b can regulate metastatic properties and EMT in breast cancer cells through miR-29b/TET1/ZEB2 signaling axis.[42] In this text, we find that MiR-29b can downregulate the expression of DNMT1 and inhibit the proliferation of EC cells.

The most common epigenetic phenomenon is DNA methylation in a CpG dinucleotide. It is catalyzed by a family of DNA methyltransferases (DNMTs) mainly consisting of three activated forms: DNMT1, DNMT3A, and DNMT3B. DNMT1 is thought to be a maintenance DNA methyltransferase that principally maintains CpG methylation.[43] The regulation of DNMT1 expression can be attributed to the following several ways: E3 ubiquitin ligase, transcription factor, epigenetics factor, and microRNA. First, E3 ubiquitin ligase RNF180 can bind directly to DNMT1 and be involved in DNMT1 degradation via ubiquitination.[44] Kindlin-2 increased the stability of DNA methyltransferase DNMT1 through interaction with DNMT1 and methylated CpG islands in the E-cadherin promoter, promoting breast cancer development.[45] Second, transcription factor ZNF479 can upregulate DNMT1 expression and promote cell proliferation and tumor growth.[46] STAT3 induces transcription of the DNA methyltransferase 1 gene (DNMT1) in malignant T lymphocytes.[47] Transcription factor TCF3 activates DNMT1 transcription and promotes glioma cell proliferation and migration.[48]

Third, PRMT6 overexpression impairs chromatin association of UHRF1, an accessory factor of DNMT1, resulting in passive DNA demethylation.[49] Sirt6 significantly promotes the acetylation of DNMT1 and stabilizes it. Consequently, acetylated DNMT1 translocates into the nucleus and methylates the Notch1 promoter region, resulting in the hindering of Notch signaling.[50] Lastly, MiR-148a-3p, by targeting DNMT1, likely regulates cell proliferation and invasion in esophageal cancer.[51] MiR-139-5p suppresses osteosarcoma cell growth and invasion through regulating DNMT1.[52] In this text, we find that miR-29b may upregulate the expression of ECRG4 by targeting DNMT1 in the EC cells.

In summary, our findings demonstrate that ECRG4 can activate IRF3/IFN-γ pathway. IFN-γ can promote the expression of miR-29b. MiR-29b reduces the expression of DNMT1. DNMT1 can affect the expression of ECRG4 affecting the methylation of ECRG4 promoter. DNMT1/ECRG4/IRF3/IFN-γ/miR-29b signaling promotes EC growth, which might contribute to tumor progression in EC, and that targeting this signaling is a potential therapeutic strategy for EC.

Limitations of the study

Our results have identified the role of ECRG4 in EC. We demonstrated that downregulation of ECRG4 by DNMT1 promotes EC growth via IRF3/IFN-γ/miR-29b/DNMT1/ECRG4 positive
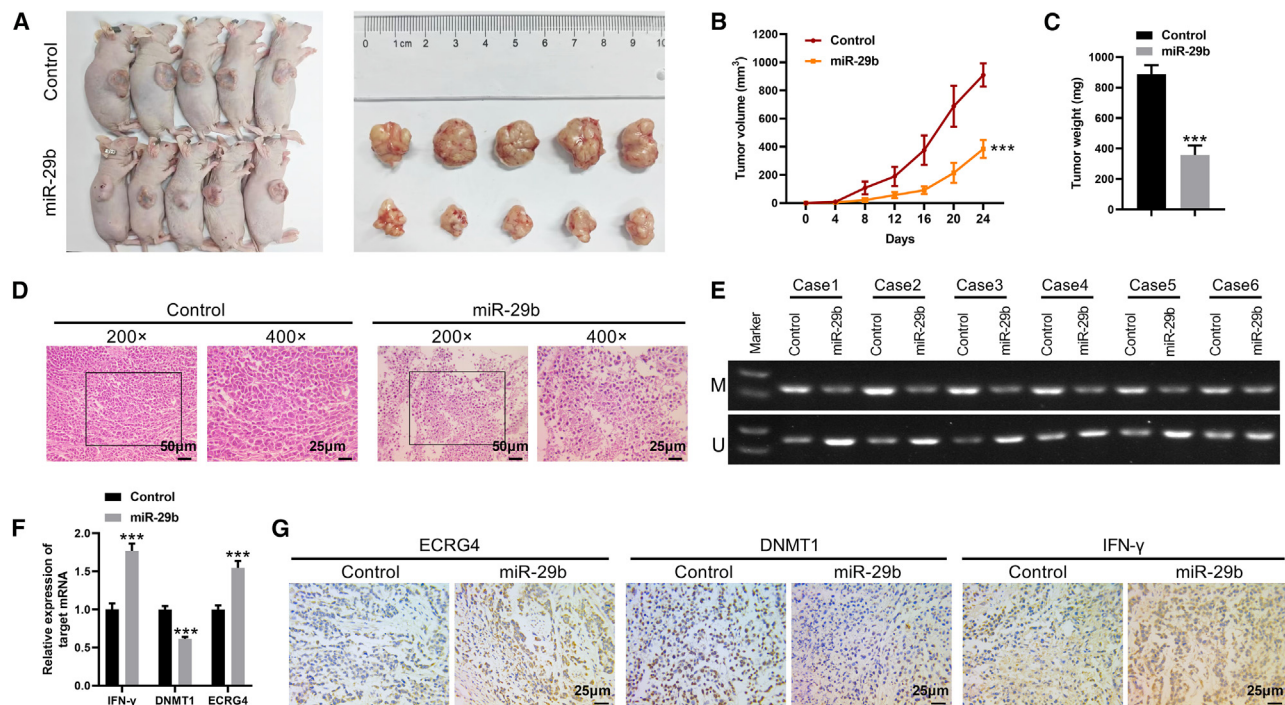
Figure 7. MiR-29b downregulates DNMT1 expression, thereby inhibiting tumor cell proliferation *in vivo*

The tumor-bearing mice then received the indicated treatment. The tumor sizes were measured on the days as indicated.

(A) Subcutaneous tumors were excised and photographs were taken at the termination of the experiment.

(B) Tumor sizes were measured on the days as indicated.

(C) Tumor weights were measured at the end of the experiments.

(D) H&E staining showed that morphology changes in tumor cells.

(E) Methylation-specific PCR was performed to evaluate the ECRG4 DNA methylation changes under miR-29b mimic treatment in EC9706 cells.

(F) qRT-PCR to measure DNMT1 and ECRG4 mRNA in the tumor specimens from the mice.

(G) Immunohistochemistry for DNMT1 and ECRG4 in the tumor specimens from the mice. The values are presented as mean ± s.d. *p* values are calculated by a two-tailed Student's *t* test. **$p < 0.01$, ***$p < 0.001$.

feedback loop. The induction of type I interferons through IRF3 is considered a major outcome of stimulator of interferon genes (STING) activation that drives immune responses against DNA viruses and tumors. Identifying the cancer immune involved in the downregulation of ECRG4 is an important area for future research.

RESOURCE AVAILABILITY

Lead contact

Further information and requests for resources and reagents should be directed to and will be fulfilled by the lead contact, Linwei Li (lilinweillw@126.com).

Materials availability statement

This study did not generate new unique reagents.

Data and code availability

- The mass spectrometry proteomics data have been deposited at the Mendeley Data, V1, with the https://doi.org/10.17632/vxnpdn6pk7.1, and are publicly available as of the data of publication. This article does not report original code.
- Any additional information required to reanalyze the data reported in this article is available from the lead contact upon request.

AUTHOR CONTRIBUTIONS

K.Y.: Conceptualization, Formal Analysis, Project Administration, Methodology, Writing – Original Draft Preparation, Writing – Review and Editing. S.Chai: Data Curation, Formal Analysis, Methodology, Writing – Original Draft Preparation, Investigation. H.S.: Formal Analysis, Methodology, Software, Validation, Visualization. S.Cao: Formal Analysis, Methodology, Data Curation. F.G.: Software, Data Curation. C.Z.: Investigation, Methodology, Data Curation. L.L.: Resources, Supervision, Funding Acquisition, Writing –Review and Editing.

DECLARATION OF INTERESTS

The authors have no conflict of interest.

STAR★METHODS

Detailed methods are provided in the online version of this paper and include the following:

- KEY RESOURCES TABLE

iScience
Article

REFERENCES

1. Sung, H., Ferlay, J., Siegel, R.L., Laversanne, M., Soerjomataram, I., Jemal, A., and Bray, F. (2021). Global Cancer Statistics 2020: GLOBOCAN Estimates of Incidence and Mortality Worldwide for 36 Cancers in 185 Countries. CA A Cancer J. Clin. *71*, 209–249. https://doi.org/10.3322/caac.21660.

2. Abnet, C.C., Arnold, M., and Wei, W.-Q. (2018). Epidemiology of Esophageal Squamous Cell Carcinoma. Gastroenterology *154*, 360–373. https://doi.org/10.1053/j.gastro.2017.08.023.

3. Niu, C., Liu, Y., Wang, J., Liu, Y., Zhang, S., Zhang, Y., Zhang, L., Zhao, D., Liu, F., Chao, L., et al. (2021). Risk factors for esophageal squamous cell carcinoma and its histological precursor lesions in China: a multicenter cross-sectional study. BMC Cancer *21*, 1034. https://doi.org/10.1186/s12885-021-08764-x.

4. Zheng, Y., Niu, X., Wei, Q., Li, Y., Li, L., and Zhao, J. (2022). Familial Esophageal Cancer in Taihang Mountain, China: An Era of Personalized Medicine Based on Family and Population Perspective. Cell Transplant. *31*, 9636897221129174. https://doi.org/10.1177/09636897221129174.

5. Chen, J.Y., Wu, X., Hong, C.Q., Chen, J., Wei, X.L., Zhou, L., Zhang, H.X., Huang, Y.T., and Peng, L. (2017). Downregulated ECRG4 is correlated with lymph node metastasis and predicts poor outcome for nasopharyngeal carcinoma patients. Clin. Transl. Oncol. *19*, 84–90. https://doi.org/10.1007/s12094-016-1507-z.

6. Tang, G.-Y., Tang, G.-J., Yin, L., Chao, C., Zhou, R., Ren, G.-P., Chen, J.-Y., and Zhang, W. (2019). ECRG4 acts as a tumor suppressor gene frequently hypermethylated in human breast cancer. Biosci. Rep. *39*, BSR20190087. https://doi.org/10.1042/bsr20190087.

7. Liang, X., Gao, J., Wang, Q., Hou, S., and Wu, C. (2020). ECRG4 Represses Cell Proliferation and Invasiveness via NFIC/OGN/NF-κB Signaling Pathway in Bladder Cancer. Front. Genet. *11*, 846. https://doi.org/10.3389/fgene.2020.00846.

8. Luo, L., Wu, J., Xie, J., Xia, L., Qian, X., Cai, Z., and Li, Z. (2016). Downregulated ECRG4 is associated with poor prognosis in renal cell cancer and is regulated by promoter DNA methylation. Tumour Biol. *37*, 1121–1129. https://doi.org/10.1007/s13277-015-3913-1.

9. You, Y., Yang, W., Qin, X., Wang, F., Li, H., Lin, C., Li, W., Gu, C., Zhang, Y., and Ran, Y. (2015). ECRG4 acts as a tumor suppressor and as a determinant of chemotherapy resistance in human nasopharyngeal carcinoma. Cell. Oncol. *38*, 205–214. https://doi.org/10.1007/s13402-015-0223-y.

10. Li, L.W., Yu, X.Y., Yang, Y., Zhang, C.P., Guo, L.P., and Lu, S.H. (2009). Expression of esophageal cancer related gene 4 (ECRG4), a novel tumor suppressor gene, in esophageal cancer and its inhibitory effect on the tumor growth in vitro and in vivo. Int. J. Cancer *125*, 1505–1513. https://doi.org/10.1002/ijc.24513.

11. Li, L.W., Li Yy Fau - Li, X.-y., Li Xy Fau - Zhang, C.-p., Zhang Cp Fau - Zhou, Y., Zhou Y Fau - Lu, S.-H., and Lu, S.H. (2011). A novel tumor suppressor gene ECRG4 interacts directly with TMPRSS11A (ECRG1) to inhibit cancer cell growth in esophageal carcinoma. BMC Cancer *11*, 1–7.

12. Nebbioso, A., Tambaro, F.P., Dell'Aversana, C., and Altucci, L. (2018). Cancer epigenetics: Moving forward. PLoS Genet. *14*, e1007362. https://doi.org/10.1371/journal.pgen.1007362.

13. Robert, M.-F., Morin, S., Beaulieu, N., Gauthier, F., Chute, I.C., Barsalou, A., and MacLeod, A.R. (2003). DNMT1 is required to maintain CpG methylation and aberrant gene silencing in human cancer cells. Nat. Genet. *33*, 61–65. https://doi.org/10.1038/ng1068.

14. Pan, T., Ding, H., Jin, L., Zhang, S., Wu, D., Pan, W., Dong, M., Ma, X., and Chen, Z. (2022). DNMT1-mediated demethylation of lncRNA MEG3 promoter suppressed breast cancer progression by repressing Notch1 signaling pathway. Cell Cycle *21*, 2323–2337. https://doi.org/10.1080/15384101.2022.2094662.

15. Liu, H., Song, Y., Qiu, H., Liu, Y., Luo, K., Yi, Y., Jiang, G., Lu, M., Zhang, Z., Yin, J., et al. (2020). Downregulation of FOXO3a by DNMT1 promotes breast cancer stem cell properties and tumorigenesis. Cell Death Differ. *27*, 966–983. https://doi.org/10.1038/s41418-019-0389-3.

16. Bai, J., Zhang, X., Hu, K., Liu, B., Wang, H., Li, A., Lin, F., Zhang, L., Sun, X., Du, Z., and Song, J. (2016). Silencing DNA methyltransferase 1 (DNMT1) inhibits proliferation, metastasis and invasion in ESCC by suppressing methylation of RASSF1A and DAPK. Oncotarget *7*, 44129–44141. https://doi.org/10.18632/oncotarget.9866.

17. Zhang, J., Chen, G.-Y., Wang, F., and Zhou, G. (2020). MiR-29b interacts with IFN-γ and induces DNA hypomethylation in CD4+ T cells of oral lichen planus. Int. J. Biol. Macromol. *147*, 1248–1254. https://doi.org/10.1016/j.ijbiomac.2019.09.252.

18. Yin, H., Jiang, Z., Wang, S., and Zhang, P. (2019). IFN-γ restores the impaired function of RNase L and induces mitochondria-mediated apoptosis in lung cancer. Cell Death Dis. *10*, 642. https://doi.org/10.1038/s41419-019-1902-9.

19. Deng, P., Chang, X.-J., Gao, Z.-M., Xu, X.-Y., Sun, A.-Q., Li, K., and Dai, D.-Q. (2018). Downregulation and DNA methylation of ECRG4 in gastric cancer. OncoTargets Ther. *11*, 4019–4028. https://doi.org/10.2147/ott.S161200.

20. Götze, S., Feldhaus, V., Traska, T., Wolter, M., Reifenberger, G., Tannapfel, A., Kuhnen, C., Martin, D., Müller, O., and Sievers, S. (2009). ECRG4 is a candidate tumor suppressor gene frequently hypermethylated in colorectal carcinoma and glioma. BMC Cancer *9*, 1–11. https://doi.org/10.1186/1471-2407-9-447.

21. Lu, J., Wen, M., Huang, Y., He, X., Wang, Y., Wu, Q., Li, Z., Castellanos-Martin, A., Abad, M., Cruz-Hernandez, J.J., et al. (2013). C2ORF40 suppresses breast cancer cell proliferation and invasion through modulating expression of M phase cell cycle genes. Epigenetics *8*, 571–583. https://doi.org/10.4161/epi.24626.

22. Huang, W., Zhou, R., Mao, L., Deng, C., and Dang, X. (2019). Esophageal cancer related gene-4 inhibits the migration and proliferation of oral squamous cell carcinoma through BC200 lncRNA/MMP-9 and -13 signaling

pathway. Cell. Signal. *62*, 109327. https://doi.org/10.1016/j.cellsig.2019.05.012.

23. Xie, Z., Li, W., Ai, J., Xie, J., and Zhang, X. (2022). C2orf40 inhibits metastasis and regulates chemo-resistance and radio-resistance of nasopharyngeal carcinoma cells by influencing cell cycle and activating the PI3K/AKT/mTOR signaling pathway. J. Transl. Med. *20*, 264. https://doi.org/10.1186/s12967-022-03446-z.

24. Dorschner, R.A.-O., Lee, J.A.-O., Cohen, O.A.-O., Costantini, T., Baird, A., and Eliceiri, B.A.-O. (2020). ECRG4 regulates neutrophil recruitment and CD44 expression during the inflammatory response to injury. Sci. Adv. *6*, eaay0518.

25. Moriguchi, T., Kaneumi, S., Takeda, S., Enomoto, K., Mishra, S.K., Miki, T., Koshimizu, U., Kitamura, H., and Kondo, T. (2016). Ecrg4 contributes to the anti-glioma immunosuveillance through type-I interferon signaling. OncoImmunology *5*, e1242547. https://doi.org/10.1080/2162402X.2016.1242547.

26. Yang, Z., Ye, X., Zhang, Y., Huang, Y., Chen, J., Zeng, Y., and Chen, J. (2022). ECRG4 acts as a tumor suppressor in nasopharyngeal carcinoma by suppressing the AKT/GSK3β/β-catenin signaling pathway. Cytotechnology *74*, 231–243. https://doi.org/10.1007/s10616-022-00520-8.

27. Yum, S., Li, M., Fang, Y., and Chen, Z.J. (2021). TBK1 recruitment to STING activates both IRF3 and NF-κB that mediate immune defense against tumors and viral infections. Proc. Natl. Acad. Sci. USA *118*, e2100225118. https://doi.org/10.1073/pnas.2100225118.

28. Fitzgerald, K.A., McWhirter, S.M., Faia, K.L., Rowe, D.C., Latz, E., Golenbock, D.T., Coyle, A.J., Liao, S.M., and Maniatis, T. (2003). IKKepsilon and TBK1 are essential components of the IRF3 signaling pathway. Nat. Immunol. *4*, 491–496. https://doi.org/10.1038/ni921.

29. Guinn, Z., Brown, D.M., and Petro, T.M. (2017). Activation of IRF3 contributes to IFN-gamma and ISG54 expression during the immune responses to B16F10 tumor growth. Int. Immunopharm. *50*, 121–129. https://doi.org/10.1016/j.intimp.2017.06.016.

30. Fang, C., Weng, T., Hu, S., Yuan, Z., Xiong, H., Huang, B., Cai, Y., Li, L., and Fu, X. (2021). IFN-gamma-induced ER stress impairs autophagy and triggers apoptosis in lung cancer cells. OncoImmunology *10*, 1962591. https://doi.org/10.1080/2162402X.2021.1962591.

31. Xu, X., Fu Xy Fau - Plate, J., Plate, J., Fau - Chong, A.S., and Chong, A.S. (1998). IFN-gamma induces cell growth inhibition by Fas-mediated apoptosis: requirement of STAT1 protein for up-regulation of Fas and FasL expression. Cancer Res. *58*, 2832–2837.

32. Zhang, Y., Ma, S., Li, T., Tian, Y., Zhou, H., Wang, H., and Huang, L. (2023). ILC1-derived IFN-gamma regulates macrophage activation in colon cancer. Biol. Direct *18*, 56. https://doi.org/10.1186/s13062-023-00401-w.

33. Xu, H., Piao, L., Wu, Y., and Liu, X. (2022). IFN-gamma enhances the anti-tumor activity of attenuated salmonella-mediated cancer immunotherapy by increasing M1 macrophage and CD4 and CD8 T cell counts and decreasing neutrophil counts. Front. Bioeng. Biotechnol. *10*, 996055. https://doi.org/10.3389/fbioe.2022.996055.

34. Robaina, M.C., Mazzoccoli, L., Arruda, V.O., Reis, F.R., Apa, A.G., de Rezende, L.M., and Klumb, C.E. (2015). Deregulation of DNMT1, DNMT3B and miR-29s in Burkitt lymphoma suggests novel contribution for disease pathogenesis. Exp. Mol. Pathol. *98*, 200–207.

35. Sur, S., Steele, R., Shi, X., and Ray, R.B. (2019). miRNA-29b Inhibits Prostate Tumor Growth and Induces Apoptosis by Increasing Bim Expression. Cells *8*, 1455. https://doi.org/10.3390/cells8111455.

36. Wang, L., Yang, L., Zhuang, T.A.-O., and Shi, X.A.-O. (2022). Tumor-Derived Exosomal miR-29b Reduces Angiogenesis in Pancreatic Cancer by Silencing ROBO1 and SRGAP2. J. Immuno. Res. *2022*, 4769385.

37. Liu, H., and Cheng, X.H. (2018). MiR-29b reverses oxaliplatin-resistance in colorectal cancer by targeting SIRT1. Oncotarget *9*, 12304.

38. Xu, W., Li, Z., Zhu, X., Xu, R., and Xu, Y. (2018). miR-29 Family Inhibits Resistance to Methotrexate and Promotes Cell Apoptosis by Targeting COL3A1 and MCL1 in Osteosarcoma. Med. Sci. Mon. Int. Med. J. Exp. Clin. Res. *24*, 8812.

39. Zhang, T., Xue, X., and Peng, H. (2019). Therapeutic Delivery of miR-29b Enhances Radiosensitivity in Cervical Cancer. Mol. Ther. *27*, 1183–1194. https://doi.org/10.1016/j.ymthe.2019.03.020.

40. Ivanovic, R.F., Viana, N.I., Morais, D.R., Silva, I.A., Leite, K.R., Pontes-Junior, J., Inoue, G., Nahas, W.C., Srougi, M., and Reis, S.T. (2018). miR-29b enhances prostate cancer cell invasion independently of MMP-2 expression. Cancer Cell Int. *18*, 18. https://doi.org/10.1186/s12935-018-0516-0.

41. Qiu, F., Sun, R., Deng, N., Guo, T., Cao, Y., Yu, Y., Wang, X., Zou, B., Zhang, S., Jing, T., et al. (2015). miR-29a/b enhances cell migration and invasion in nasopharyngeal carcinoma progression by regulating SPARC and COL3A1 gene expression. PLoS One *10*, e0120969.

42. Wang, H., An, X., Yu, H., Zhang, S., Tang, B., Zhang, X., and Li, Z. (2017). MiR-29b/TET1/ZEB2 signaling axis regulates metastatic properties and epithelial-mesenchymal transition in breast cancer cells. Oncotarget *8*, 102119.

43. Li, H., Li, W., Liu, S., Zong, S., Wang, W., Ren, J., Li, Q., Hou, F., and Shi, Q. (2016). DNMT1, DNMT3A and DNMT3B Polymorphisms Associated With Gastric Cancer Risk: A Systematic Review and Meta-analysis. EBioMedicine *13*, 125–131.

44. Zhang, N., Gao, X., Yuan, Q., Fu, X., Wang, P., Cai, F., Liu, H., Zhang, J., Liang, H., Nie, Y., and Deng, J. (2023). E3 ubiquitin ligase RNF180 prevents excessive PCDH10 methylation to suppress the proliferation and metastasis of gastric cancer cells by promoting ubiquitination of DNMT1. Clin. Epigenet. *15*, 77.

45. Wang, P., Chu, W., Zhang, X., Li, B., Wu, J., Qi, L., Yu, Y., and Zhang, H. (2018). Kindlin-2 interacts with and stabilizes DNMT1 to promote breast cancer development. Int. J. Biochem. Cell Biol. *105*, 41–51.

46. Wu, Y.J., Ko, B.S., Liang, S.M., Lu, Y.J., Jan, Y.J., Jiang, S.S., Shyue, S.K., Chen, L., and Liou, J.Y. (2019). ZNF479 downregulates metallothionein-1 expression by regulating ASH2L and DNMT1 in hepatocellular carcinoma. Cell Death Dis. *10*, 408. https://doi.org/10.1038/s41419-019-1651-9.

47. Zhang, Q., Wang, H.Y., Woetmann, A., Raghunath, P.N., Odum, N., and Wasik, M.A. (2006). STAT3 induces transcription of the DNA methyltransferase 1 gene (DNMT1) in malignant T lymphocytes. Blood *108*, 1058–1064. https://doi.org/10.1182/blood-2005-08-007377.

48. Zeng, W., Jiang, H., Wang, Y., Wang, C., and Yu, B.A.-O. (2022). TCF3 Induces DNMT1 Expression to Regulate Wnt Signaling Pathway in Glioma. Neurotoxicity Research *40*, 721–732.

49. Veland, N., Hardikar, S., Zhong, Y., Gayatri, S., Dan, J., Strahl, B.D., Rothbart, S.B., Bedford, M.T., and Chen, T. (2017). The Arginine Methyltransferase PRMT6 Regulates DNA Methylation and Contributes to Global DNA Hypomethylation in Cancer. Cell Rep. *21*, 3390–3397. https://doi.org/10.1016/j.celrep.2017.11.082.

50. Subramani, P., Nagarajan, N., Mariaraj, S., and Vilwanathan, R. (2023). Knockdown of sirtuin6 positively regulates acetylation of DNMT1 to inhibit NOTCH signaling pathway in non-small cell lung cancer cell lines. Cellular Signalling *105*, 110629.

51. Wang, Y., Hu, Y., Guo, J., and Wang, L. (2019). miR-148a-3p Suppresses the Proliferation and Invasion of Esophageal Cancer by Targeting DNMT1. Genet. Test. Mol. Biomarkers *23*, 98–104. https://doi.org/10.1089/gtmb.2018.0285.

52. Shi, Y.K., and Guo, Y.H. (2018). MiR-139-5p suppresses osteosarcoma cell growth and invasion through regulating DNMT1. Biochem. Biophys. Res. Commun. *503*, 459–466. https://doi.org/10.1016/j.bbrc.2018.04.124.

STAR★METHODS

KEY RESOURCES TABLE

REAGENT or RESOURCE	SOURCE	IDENTIFIER
Antibodies		
ECRG4	Gene Tex	GTX87799; RRID:AB_10734114
IRF3	Abcam	ab68481; RRID:AB_11155653
p-IRF3/S386	Boster	BM4844
IFN-γ	Gene Tex	GTX15750
DNMT1	Cell signaling technology	5032; RRID:AB_10548197
GAPDH	Cell signaling technology	2118; RRID:AB_561053
Virus strains		
Lv-ECRG4	Gene Chem Co., Ltd	N/A
Lv-miR-29b	Gene Chem Co., Ltd	N/A
Biological sample		
Fresh esophageal carcinoma tissues	Henan Provincial People's Hospital	N/A
Chemicals and recombinant proteins		
5-Azacytidine	Selleck	S1782
Lipofectamine 2000	Invitrogen	11668500
Recombinant Human IFN-γ Protein	R&D Corporation	285-IF-100/CF
Critical commercial assays		
Chip kit	Abcam	ab117152
Apoptosis analysis kit	BD	556547
DNA extraction kit	Omega	D5032-02
EZ DNA Methylation kit	Zymo Research	D5002
DNA Methylation Elisa Easy kit	Epi Gentek	P-1030-48
Epi Quik Nuclear Extraction kit	Epi Gentek	OP-0002-1
Deposited data		
proteomics data	This paper	https://doi.org/10.17632/vxnpdn6pk7.1.
Experimental models: cell line		
HEEC	Xiamen Yi mo Biotechnology	IM-H467
EC9706	Shanghai EK-Bioscience	CC-Y1571
EC18	Shanghai Xin Yu Biotech	XY0573
Experimental models: mouse		
BALB/c-nu mice	SPF (Beijing) Biotechnology	N/A
Oligonucleotides		
ECRG4 forward: 5′-CCGGTCTC CCTCGCAGCAC-3′	Sangon	N/A
ECRG4 reverse: 5′-CGCTTCTG GCGCTTCGGCT-3′	Sangon	N/A
DNMT1 forward: 5′-AACCTTCA CCTAGCCCAG-3	Sangon	N/A
DNMT1 reverse: 5′-CTCATCCGA TTTGGCTCTTTCA-3′	Sangon	N/A
IFN-γ forwad: 5′-CTGGAGGAA CTGGCAAAGG-3′	Sangon	N/A
IFN-γ reverse: 5′-CTGGACCTGT GGGTTGTTGA-3′	Sangon	N/A
IRF3 forward: 5′-AGGAGCTGTT AGAGATGG-3′	Sangon	N/A

(Continued on next page)

Continued

REAGENT or RESOURCE	SOURCE	IDENTIFIER
IRF3 reverse: 5′-TACTGGTCAG AGGTAAGG-3′	Sangon	N/A
GAPDH forward: 5′-GTCGGTGTGA ACGGATTTG-3′	Sangon	N/A
GAPDH reverse: 5′-TCCCATTCTC AGCCTTGAC-3′	Sangon	N/A
miR-29b forward: 5′-TCGGTCCAG TTTTCCCAG-3′	Sangon	N/A
miR-29b reverse:5′-AGTGCGTG TCGTGGAGTC-3′	Sangon	N/A
U6 forward: 5′-TGCGGGTGCT CGCTTCGGCAGC-3′	Sangon	N/A
U6 reverse: 5′-CCAGTGCAG GGTCCGAGGT-3′	Sangon	N/A
ECRG4 forward (for chip): 5′-GAA TTGAAGCTTGGCCCACG-3′	Sangon	N/A
ECRG4 reverse (for chip): 5′-GCGGC AGTG TGCTGCAAAGT-3′	Sangon	N/A
ECRG4 forward (M): 5′-TGGCGTT TTTATGGTGTTC-3′	Sangon	N/A
ECRG4 reverse (M): 5′-CACCACTT CGCACTTATACG-3′	Sangon	N/A
ECRG4 forward (U): 5′-ATGTGGTGT TTTTATGGTGTTT-3′	Rib Bio	N/A
ECRG4 reverse (U): 5′-AAACACCAC TTCACACTTATACA-3′	Rib Bio	N/A
IRF3 siRNA(1):5′-AGACAUUCUGG AUGAGUUA-3′	Rib Bio	N/A
RF3 siRNA(2): 5′-CCCUUCAUUG UAGAUCUGATT-3′		
IRF3 siRNA(3):5′-GGTTGTTCCTA CATGTCTTAA-3		
Recombinant DNA		
pcDNA3.1-ECRG4 plasmid	Gene chem	
Software		
GraphPad Prism 8.0 software	GraphPad Prism Software Inc.	https://www.graphpad.com

EXPERIMENTAL MODEL AND STUDY PARTICIPANT DETAILS

Patients and clinical specimens

All patient samples were collected from Zhengzhou University with written informed consent. The ethical approval was granted from the Committees for Ethical Review of Zhengzhou University. Pathological diagnosis was made according to the histology of tumor specimens or biopsy and examined by experienced pathologists. Esophageal carcinoma tissues and adjacent normal tissues were stored in liquid nitrogen. The study is compliant with all relevant ethical regulations for human research participants, and all participants signed informed consent forms.

Cell lines and culture

The esophageal epithelial cells HEEC and esophageal carcinoma cancer cell line EC9706, EC-18 were grown in 89% RPMI 1640 (Gibco, Grand Island, USA), with 10% FBS (Gibco) and+1% Penicillin-Streptomycin medium (Sigma-Aldrich, St. Louis, USA). Cells were maintained at 37°C in a humidified 5% CO_2 incubation.

Xenograft assays in nude mice

Animal studies were approved by the Ethics Committee of Zhengzhou University, and the animal protocol was in accordance with the institutional guidelines of the Animal Care and Use Committee of Zhengzhou University. The EC9706 cells or EC-18 cells were injected subcutaneously into female nude mice (2×10^6 cells in 100 μL per inoculation) Tumor volume was calculated as length×

width2× (π/6). When the tumors were palpable, mice were alternately divided into two groups When the mean diameter of tumors reached 5–6 mm, the mice received indicated treatment. Tumor sizes and body weights were measured every 4 days.

METHOD DETAILS

Reagents and antibodies

The following antibodies were used: anti-ECRG4 (Gene Tex, No. GTX87799), anti-IRF3 (Abcam, No. ab68481), Anti-p-IRF3/S386 (Boster, No. BM4844) anti-IFN-γ (Gene Tex, No. GTX15750) anti-DNMT1 (CST, No 5032), anti-GAPDH (CST, No. 2118). Normal IgG/Peroxidase-conjugated Affini Pure Goat Anti-Rabbit/Mouse IgG (H + L) was purchased from Jackson Immuno Research. Recombinant Human IFN-gamma Protein (No. 285-IF-100/CF) was purchased from R&D Corporation (Minneapolis, USA). The recombinant plasmid pcDNA3.1-ECRG4 was constructed by Gene chem (Shanghai, China). miRNA mimics, small interfering RNAs (siRNAs) were purchased from Rib Bio (Guangzhou, China). 5-Azacytidine was purchased from Selleck (Houston, USA).

Cell transfection

Transfection of miRNA mimics, small interfering RNAs (siRNAs) and plasmid were performed using Lipofectamine 2000 (Invitrogen, Carlsbad, USA) according to the manufacturer's protocol. Briefly, cells in the exponential phase of growth were plated in six-well tissue culture plates at 1×10^5 cells per well, grown for 24 h, and then transfected with siRNA or plasmids using Lipofectamine 2000 reagent. EC9706 grown to 70–80% confluence was infected with an ECRG4 lentivirus (or miR-29b lentivirus) in the presence of Polybrene (8 μg/ml). After 48h, we determined lentiviral infection efficiency based on green fluorescent protein (GFP) expression. The stably transfected cells were selected and enriched using puromycin (2 μg/mL). IRF3 siRNA are as follows: sequence 1: 5′-AGA CAUUCUGGAUGAGUUA-3′, sequence 2: 5′-CCCUUCAUUGUAGAUCUGAUU-3′, sequence 3: 5′-GGUUGUUCCUACAUGUCUU AA-3′.

Proteomic analysis

Proteomic analysis was conducted with the method in this article.[17] Briefly,EC9706 cells were transduced with ECRG4 expressing lentivirus and harvested for proteomic analysis. An equal amount of about 100 μg of protein is reduced, alkylated, and precipitated by acetone. The precipitate was re-suspended in 200mm tetraethyl ammonium bromide (TEAB) and then digested with trypsin. The peptides in the Control group were labeled with MTT-126, MTT-127N and MTT-128N, while the peptides of ECRG4 overexpression group were labeled with MTT-129N, MTT-130N and MTT-131N. The obtained sample were remixed by high-performance liquid chromatography (HPLC) and the results were analyzed by LC-MS/MS. MS raw data was analysised with Proteome Discoverer software version 2.1 (Thermo Fisher Scientific).

Quantitative real-time RT-PCR (qRT-PCR) for mRNA

Total RNA was isolated using Trizol reagent (Invitrogen) according to manufacturers' protocols. cDNA was synthesized by using Prime Script RT reagent kit (Takara, Shiga, Japan) according to manufacturers' protocols. Quantity real-time PCR was performed using iTap universal SYBR Green (Bio-rad, Hercules, USA), and was run on CFX96 system (Bio-Rad). For quantification of gene expression, the $2^{-\Delta\Delta Ct}$ method was used. GAPDH expression was used for normalization. The primers were used as follows: ECRG4 forward: 5′-CCGGTCTCCCTCGCAGCAC-3′, ECRG4 reverse: 5′-CGCTTCTGGCGCTTCGGCT-3′; DNMT1 forward: 5′-AACCTTCACCTAGCCCAG-3′; DNMT1 reverse: 5′-CTCATCCGATTTGGCTCTTTCA-3′; IFN-γ forwad: 5′-CTGGAGGAACTGGCA AAGG-3′, IFN-γ reverse: 5′-CTGGACCTGTGGGTTGTTGA-3′, IRF3 forward:5′-AGGAGCTGTTAGAGATGG-3′, IRF3 reverse: 5′-TACTGGTCAGAGGTAAGG-3′; GAPDH forward: 5′-GTCGGTGTGAACGGATTTG-3′, GAPDH reverse: 5′-TCCCATTCTCAG CCTTGAC-3′.

Quantitative real-time RT-PCR (qRT-PCR) micro RNA

QRT-PCR was also performed to analyze the expression levels of mature microRNAs using Prime Script miRNA RT-PCR Kit (Takara) following the manufacturer's protocols. miRNA expressions were tested using SYBR Green qPCR (Takara) assay. The Comparative cycle threshold (Ct) method was used to calculate the relative abundance of microRNA normalized to U6. The primer sequences used were as follows: miR-29b forward: miR-29b forward: 5′-TCGGTCCAGTTTTCCCAG-3′, miR-29b reverse: 5′-AGTGCGTGTCGTG GAGTC-3′; U6 forward: 5′-TGCGGGTGCTCGCTTCGGCAGC-3′, U6 reverse: 5′-CCAGTGCAGGGTCCGAGGT-3′. U6 served as an internal reference.

Immunohistochemistry (IHC)

Immunohistochemical assay was performed on formalin fixed, paraffin-embedded sections of clinical esophageal carcinoma tissues or xenograft mice tissues. Briefly, the sections were deparaffinized in xylene (Aladdin regents, Shanghai, China), rehydrated with graded alcohol, and antigen retrieval was performed for 10 min in 0.01 M citrate-buffer (pH 6.0) in a pressure cooker. The slides were incubated in 3% H2O2 for 15 min and 80% carbinol for 30 min. Sections for immunohistochemistry staining were blocked for nonspecific binding by incubation in normal goat serum (ZSGB bio, No. ZLI-9056) at room temperature. Subsequently, slides were incubated with a primary antibody at 4 °C overnight. After washing again, the slides were processed with HRP conjugated

secondary antibody for 1 h at room temperature followed by 3,3-diaminobenzidine (DAB) solution (ZSGB bio, No. ZLI-9017). Next, slides were then counterstained with hematoxylin. After counterstaining with hematoxylin, the slides were dehydrated and sealed with neutral resin.

Immunofluorescence (IF)

Esophageal carcinoma Cells were fixed in 4% paraformaldehyde and permeabilized with 0.2% Triton X-100. After blocking, the cells were incubated with primary antibodies anti-IRF3 (Abcam, No ab68481), and then a fluorescent secondary antibody. Finally, the nuclei were labeled with DAPI (CST, Denvers, USA) for 15 min. Images were captured by the BX41 microscope (Olympus, Tokyo, Japan). All experiments were performed in triplicate.

The tissue sections were deparaffinized in xylene (Aladdin regents, Shanghai, China), and rehydrated with graded alcohol, Antigen retrieval was performed for 10 min in 0.01 M citrate buffer (pH 6.0) in a pressure cooker. The slides were incubated in 3% 'H$_2$O$_2$ for 15 min and 80% carbinol for 30 min. Sections for Immunofluorescence staining were blocked for nonspecific binding by incubation in normal goat serum (ZSGB bio, No. ZLI-9056) at room temperature. After blocking, the cells were incubated with primary antibodies anti-ECRG4 (Gene Tex, No. GTX87799), and then a fluorescent secondary antibody. Finally, the nuclei were labeled with DAPI (CST, Denvers, USA) for 15 min. Images were captured by the BX41 microscope (Olympus, Tokyo, Japan). All experiments were performed in triplicate.

Elisa assay for IFN-γ

The concentration of IFN-γ in the supernatant of the cell culture was examined by Elisa kit (R&D, No. QK285) conforming to the manufacture's instruction.

Hematoxylin and eosin staining (H&E staining)

The tumor section was cut conventionally and were stained with hematoxylin and eosin (Solarbio, No, G1120). The stained sections were dehydrated with ethanol and transparently dried with xylene, which were then placed under a microscope (100×) and photographed.

Cell proliferation assay

The capacity of cellular proliferation was measured using the Cell Counting Kit 8 (Bimake, Shanghai, China) according to the manufacturer's instructions. Esophageal carcinoma cells were harvested after 24 h transfection and re-seeded onto 96 well plates at a density of 3000 cells per well. The optical density was determined with a microplate reader at a wavelength of 450 nm. Each assay was performed in triplicate and independently repeated three times. Treated cells were seeded at 800/well in the same six-well plates. After colony formation, the cells were washed with PBS and immobilized by 4% formaldehyde at room temperature for 30 min. Finally, the cells were dyed with 0.5% crystal violet for 30 min.

Flow cytometry

For apoptosis analysis, cells were analyzed with FITC Annexin V Apoptosis Detection Kit I (BD. No. 556547). After the treatment, cells were harvested and rinsed with cold PBS twice by centrifugation at 1000×g and resuspended in 100 μL of binding buffer. Next, 5 μL of Annexin-V and 5 μL of PI were added to the solution and incubated for 15 min at room temperature in the dark for flow cytometric analysis (Beckman Coulter, Brea, USA). Each experiment was repeated three times.

Western blotting

Cells were lysed with RIPA buffer (Beyotime, Haimen, China) supplemented with a phosphatase inhibitor cocktail and a protease inhibitor cocktail (Selleck, Houston, USA). Protein concentrations of the lysates were determined by BCA assay kit. 30 μg of protein were separated by SDS-PAGE and transferred to PVDF membranes. The membranes were blocked with 5% skim milk in PBST. The membranes were incubated with primary antibodies overnight and then peroxidase-conjugated secondary antibodies at room temperature for 1 h. Finally, the membranes were visualized by using ECL detection system (Bio-rad, Hercules, USA) with an enhanced chemiluminescent detection kit. The blots were analyzed using the ImageJ program.

Methylation-specific polymerase chain reaction (MSP)

Genomic DNA was harvested with a DNA extraction kit (Omega, No. D5032-02). 2 μg was used for bisulfite modification via the EZ DNA Methylation kit (Zymo Research, No. D5002). The primers of ECRG4 for methylated sequences were 5′-TGGCGTTTT TATGGTGTTC-3′and 5′-CACCACTTCGCACTTATACG-3′, generating a 137-bp PCR product. The primers of ECRG4 for unmethylated sequences were 5′-ATGTGGTGTTTTTATGGTGTTT-3′and 5′-AAACACCACTTCACACTTATACA-3′, generating another 137 bp PCR product. For PCR, the total reaction volume was 50 μL, and the mixture contained DNA, sense and antisense primers, 10 × Dream Taq buffer, dNTP mix, and Dream Taq DNA polymerase. The reaction conditions were as follows: predenaturation at 95°C for 5 min, followed by 34 cycles at 95°C for 30 s, 62°C for 30 s, and 72°C for 30 s, with a final extension at 72°C for 10 min. The PCR products were subjected to agarose gel electrophoresis at 120 V for 40 min. The gels were photographed by using an electrophoretic gel imaging analysis system.

Chromatin immunoprecipitation assay

The chromatin or DNA-protein complex was isolated using Chromatin Extraction Kit according to the manufacturer's instruction (Abcam, ab117152). Then Chromatin immunoprecipitation (ChIP) experiment was carried out using ChIP Kit-One Step according to the manufacturer's instructions (Abcam, ab117138). Quantitative real-time PCR (qRT-PCR) was performed to test the ChIP signal, and enrichment of target was analyzed. The follow antibodies were used: DNMT1(CST, No.5032), DNMT3a (CST, No. 49768), DNMT3b (CST, No. 57868). The following specific primers were used in the ChIP-qPCR analysis: ECRG4 forward: 5′-GAATTG AAGCTTGGCCCCACG-3′, ECRG4 reverse: 5′-GCGGCAGTG TGCTGCAAAGT-3′.

Global DNA methylation assay

Global methylation levels of cell DNA were evaluated through the Methyl Flash Global DNA Methylation Elisa Easy kit (Epigentek, No. P-1030-48). Briefly, about 100 ng of genomic DNA was used for 5-methylcytosine (5-mC) quantitate on. The genomic DNA was added to microplate well with a high affinity for DNA binding. After the standard incubation and washing, 5-mC detection complex solution was added to the plate. The samples were read colorimetrically on an automated plate reader at 450 nm absorbance. DNA methylation was calculated as follows:

$$5mC\% = \frac{Sample\ OD - NC\ OD}{Slope \times inputDNA\ amount\ (ng)} \times 100$$

Measurement of DNMT activity

Nuclear extracts containing were obtained through the EpiQuik Nuclear Extraction kit (EpiGentek, No. OP-0002-1). After protein quantification with Total Protein Kit (Micro Lowry) (Sigma-Aldrich, No. TP0200-1KT), 12 μg of nuclear protein was used to measure total DNMT activity with the EpiQuik DNA Methyltransferase (DNMT) Activity/Inhibition Assay Kit (Epigentek, No. P-3001-1) in accordance with the manufacturer's instructions.

QUANTIFICATION AND STATISTICAL ANALYSIS

Data analysis was performed using GraphPad Prism 8.0 software. The difference between the two group samples was analyzed using unpaired two-tailed Student's t test. Comparison of multiple groups (>2) were conducted using one or two-way ANOVA with Tukey's post hoc analysis. The results are shown as the mean ± s.d. All experiments were performed at least three times. $p < 0.05$ was considered statistically significant.